

Influence of the nature of the noble metal (Rh,Pt) on the low-temperature reducibility of a Ce/Tb mixed oxide with application as TWC component

G. Blanco,^{1*} J. M. Pintado,¹ S. Bernal,¹ M. A. Cauqui,¹ M. P. Corchado,¹ A. Galtayries,² J. Ghijsen,³ R. Sporken,³ T. Eickhoff⁴ and W. Drube⁴

¹ Departamento de Ciencia de los Materiales e Ingeniería Metalúrgica y Química Inorgánica, Facultad de Ciencias, Universidad de Cádiz, Apartado 40, E-11510 Puerto Real (Cádiz), Spain

² Laboratoire de Physico-Chimie des Surfaces, ENSCP, 11 rue Pierre et Marie Curie, F-75231 Paris Cedex 05, France

³ Laboratoire Interdisciplinaire de Spectroscopie Electronique (LISE), Facultés Universitaires Notre-Dame de la Paix, rue de Bruxelles 61, B-5000 Namur, Belgium

⁴ Hasylab am DESY, Hamburg, Germany

Received 16 July 2001; Revised 6 December 2001; Accepted 3 January 2002

Ceria-based mixed oxides have proved to be good alternatives to pure ceria as redox materials for advanced three-way catalysts. In this work, the behaviour of a $\text{Ce}_{0.8}\text{Tb}_{0.2}\text{O}_{2-x}$ mixed-oxide sample and the corresponding oxide-supported Rh and Pt samples has been investigated. Special attention has been paid to the low-temperature redox response. Temperature-programmed desorption (TPD), temperature-programmed reduction and oxygen buffering capacity were used as experimental techniques. The evolution of reducibility was also followed by tunable high-energy x-ray photoemission spectroscopy, focussing on the surface information provided by Tb 3d and Ce 3d core levels. The oxidation state of both Ce and Tb was followed during ultrahigh vacuum annealing of the three samples up to 750 K. Comparison of the XPS spectra for the different samples before and after annealing showed that the Ce^{4+} reduction was negligible but Tb^{4+} was gradually reduced to Tb^{3+} . Furthermore, the TPD and XPS experiments are in good agreement, with the highest reduction rate corresponding to the Rh/CeTbO_x sample. Copyright © 2002 John Wiley & Sons, Ltd.

KEYWORDS: THE-XPS; oxygen buffering capacity; cerium/terbium mixed oxides; noble metals; TWC

INTRODUCTION

During the last 20 years, efforts made on the investigation of ceria-based catalytic materials have rapidly increased.¹ Most of them are devoted to noble metals (Pt, Pd, Rh) supported on ceria and ceria-based materials, owing to the close relationship between these oxides and catalysts used to control exhaust emissions from motor vehicles.^{2–6} In latter years, the interest on ceria-supported metals has been shifted progressively towards mixed-oxide-supported catalysts. Alternative ceria-containing mixed oxides with fluorite-related structure^{2,3,6} started to be investigated at the beginning of the last decade as alternative oxygen storage materials. Nowadays, ceria–zirconia materials are used in the latest generation of automotive three-way catalysts (TWCs).

Some investigations have shown that the incorporation of praseodymium^{7–9} or terbium^{10–13} ions into the ceria lattice

improves its redox properties very significantly, being, such materials thus having potential interest as components in TWCs as well as in other applications. This interest is related to their high oxygen storage capacity and oxygen buffering capacity (OBC), i.e. their ability to release or uptake oxygen under reducing or oxidizing conditions. On the other hand, for sufficiently high reduction temperatures an inhibition of the chemisorptive capacity of the supported metal is known to occur, this phenomenon being associated with reducible supports.¹⁴ The relationship between the support reduction and catalyst deactivation phenomena is an important reason to investigate the actual redox state of these supports.

Cerium/terbium mixed oxides cannot be reoxidized to the dioxide ($\text{Ce}_x\text{Tb}_{1-x}\text{O}_2$).¹⁵ The actual composition of $\text{Ce}_x\text{Tb}_{1-x}\text{O}_{2-y}$, even in oxidized samples, depends on several factors including temperature and oxygen pressure,^{16,17} therefore determination of the actual reduction degree cannot be established by means of oxidation in pulses and TPO (Thermal Programmed Oxidation) as applied in Ref. 18. A Faraday magnetic balance seems to be very useful in ceria-supported catalysts but, owing to the presence of terbium together with ceria, it is not possible to apply this technique. Moreover, when studying rare-earth compounds by XPS,

*Correspondence to: G. Blanco, Departamento de Ciencia de los Materiales e Ingeniería Metalúrgica y Química Inorgánica, Facultad de Ciencias, Universidad de Cádiz, Apartado 40, E-11510 Puerto Real (Cádiz), Spain. E-mail: ginesa.blanco@uca.es
Contract/grant sponsor: CICYT; Contract/grant number: MAT99-0570.

only a few papers can be found in the literature. Amongst the lanthanides, cerium is the most widely investigated element, and thus in the literature there are papers dealing with theoretical^{19,20} and experimental aspects.^{21–25} However, as far as terbium studies are concerned, very few data can be found in the literature.^{19–22} All these spectra are very complex and thus their interpretation has required extensive work. In spite of this, XPS can provide information about the reduction degree of each of the two lanthanides present in the mixed oxide.

EXPERIMENTAL

The cerium–terbium mixed oxide studied in this work, $\text{Ce}_{0.8}\text{Tb}_{0.2}\text{O}_x$, was prepared by co-precipitation of the corresponding nitrates with ammonia. The dried precipitate was calcined in air at 873 K for 2 h and finally calcined under $\text{O}_2(5\%)/\text{He}$ at 1173 K for 2 h. The Ce/Tb molar ratio of the resulting mixed oxide was 80:20. The oxide-supported Rh and Pt samples were prepared by incipient wetness impregnation with an aqueous solution of $\text{Rh}(\text{NO}_3)_3$ in the case of Rh/CeTbO_x and with $[\text{Pt}(\text{NH}_3)_4](\text{OH})_2$ for Pt/CeTbO_x. Metal loadings were 0.5 wt.% for Rh catalyst and 1 wt.% for Pt catalyst. Prior to all the experiments, the samples were pretreated in a flow of $\text{O}_2(5\%)/\text{He}$ at 773 K for 1 h, cooled slowly to 373 K under the oxidizing mixture and then to room temperature in pure He. This standard pretreatment guarantees a common well-defined starting redox state for each sample throughout the whole study.

Temperature-programmed Desorption (TPD) and temperature-programmed Reduction (TPR) experiments were performed in a flow of He or $\text{H}_2(5\%)/\text{Ar}$, respectively, the flow rate being 60 ml min^{-1} and the heating rate 10 K min^{-1} . The experiments were performed with a VG Sensorlab 200D mass spectrometer as the analytical device. The experimental method for OBC measurements has been described elsewhere.¹² Briefly, it consists of the injection of 0.25 ml of $\text{O}_2(5\%)/\text{He}$ pulses at 10 s intervals in a 60 ml min^{-1} He stream. The oscillations produced by this continuous pulsing of O_2 can be buffered by an active sample by consuming or releasing oxygen in the high P_{O_2} or low P_{O_2} period of the pulse, respectively. The experiments were monitored with a thermal conductivity detector. Two sets of experiments were performed: isothermal OBC and temperature-programmed OBC.

Tunable high-energy x-ray photoemission spectroscopy (THE-XPS) was performed in a Scienta 200 analyser placed in the beamline BW2 at Hasylab. A photon energy of 3000 eV was used, giving a mean free path of $\sim 70 \text{ \AA}$ for the photoemitted electrons. This λ value has been calculated as proposed by Cumson and Seah²⁶ by using density values for Tb 3d in Tb_2O_3 . The analysed depth was then estimated to be $\sim 280 \text{ \AA}$ for Tb 3d and Ce 3d core levels ($\sim 4\lambda$). The resolution was 0.8 eV on Ag 3d_{3/2}. Charge effects were compensated by using a copper grid placed over the pressed samples. The analyser was equipped with a device for *in situ* heating of the samples under vacuum to a temperature up to 750 K.

RESULTS AND DISCUSSION

TPD and TPR studies

Figure 1(A) shows the TPD experiments performed on CeTbO_x (trace a), Pt/CeTbO_x (trace b) and Rh/CeTbO_x (trace c). Both TPD curves corresponding to CeTbO_x and Pt/CeTbO_x samples are very similar, consisting of a main peak centred at $\sim 623 \text{ K}$ followed by a broad reduction signal that extends to 1223 K. For both samples, the reduction process starts to be noticeable at a temperature of $\sim 473 \text{ K}$. For the Rh/CeTbO_x catalyst, the TPD trace is different (Fig. 1(A,c)), consisting of a first reduction feature centred at 430 K, with an overlapping peak at slightly higher temperature, followed by a broad peak similar to that of CeTbO_x and Pt/CeTbO_x samples.

Figure 1(B) depicts the TPR traces for the samples. In the case of CeTbO_x (trace a), water evolution starts at 573 K, with a main reduction peak centred at 673 K and a second broad feature at much higher temperature ($\sim 1000 \text{ K}$). When a noble metal, Pt or Rh, is supported on the mixed oxide, a great improvement of reducibility can be observed (Fig 2(B,b) and 2(B,c)). The main peak of the mixed oxide is then shifted towards extremely low temperatures, slightly above room temperature.

From comparison of the TPD and TPR traces for all the samples, it seems that supporting rhodium on the mixed oxide can enhance its reducibility when reducing under inert gas or hydrogen. Supporting platinum, however, only enhances the reducibility of the sample when reducing under hydrogen, but not under inert gas. Nevertheless, from the TPD or TPR it is not possible to determine the origin of the evolving species, oxygen or water, respectively. For the samples studied here, the reduction can come from the $\text{Ce}^{3+}/\text{Ce}^{4+}$ couple, from the $\text{Tb}^{3+}/\text{Tb}^{4+}$ couple and/or from the reduction of an oxide of the noble metal that could be formed during the oxidizing pretreatment. To identify which are the species involved in the reduction process, another analysis technique, different from TPD or TPR, should be

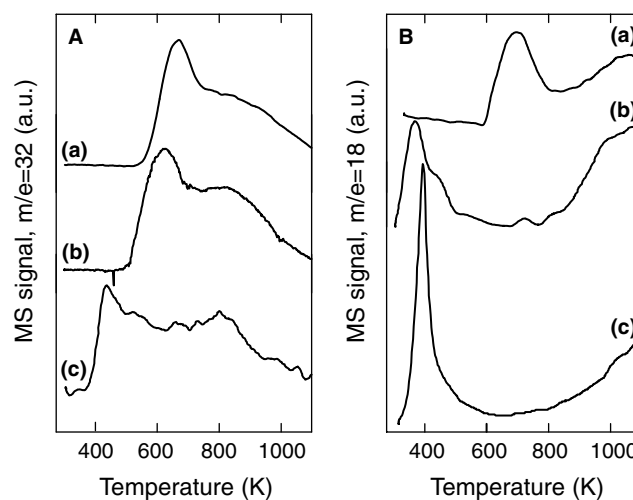


Figure 1. The TPD (A) and TPR (B) traces corresponding to CeTbO_x (curves a), Pt/CeTbO_x (curves b) and Rh/CeTbO_x (curves c).

applied. Later in this paper, results obtained by XPS will be discussed.

OBC experiments

Two types of experiments were performed on the samples: temperature-programmed OBC (Fig. 2), to establish the starting temperature for the samples to be effective as oxygen buffers; and isothermal OBC experiments, to measure the OBC value at selected temperatures (Table 1).

Thus, the samples were submitted to the temperature-programmed OBC experiments shown in Fig. 2. As can be seen, the results are in good agreement with TPD data, the behaviour of CeTbO_x (Fig. 2(a)) and Pt/CeTbO_x (Fig. 2(b)) being quite similar. The oscillations start to be buffered effectively at 500–550 K, reaching a maximum value from

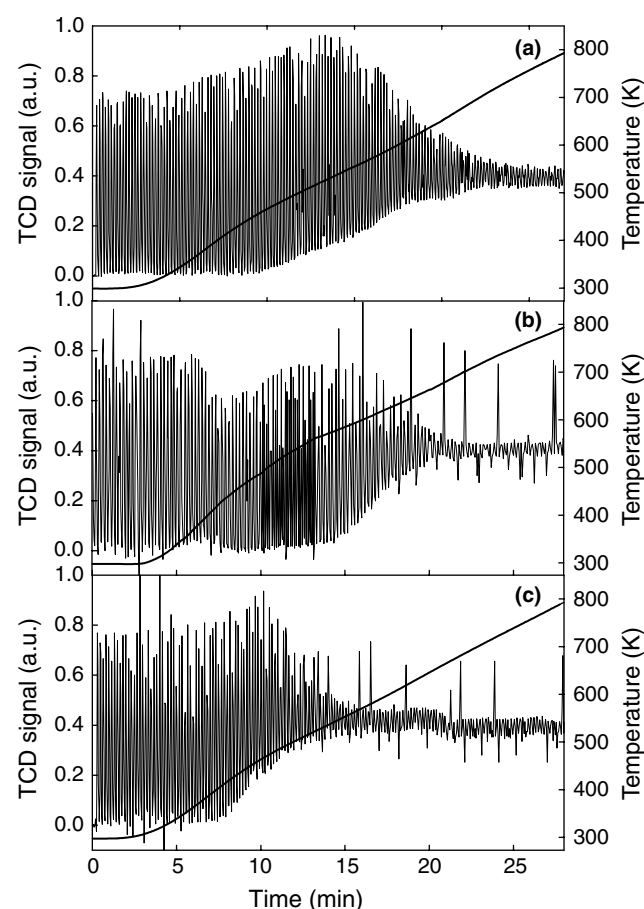


Figure 2. Temperature-programmed OBC experiments corresponding to CeTbO_x (a), Pt/CeTbO_x (b) and Rh/CeTbO_x (c).

Table 1. Oxygen buffering capacity (%) under isothermal conditions for the samples studied

| Temperature (K) | Sample | | |
|-----------------|--------------------|-----------------------|-----------------------|
| | CeTbO _x | Pt/CeTbO _x | Rh/CeTbO _x |
| 473 | 0 | 1 | 36 |
| 573 | 1 | 4 | 84 |
| 673 | 44 | 38 | 95 |
| 773 | 93 | 93 | 95 |

650 K. For Rh/CeTbO_x (Fig. 2(c)) it can be seen that there is again a different behaviour, the sample starting to be active at 450 K. The maximum values of the OBC seem to be similar for the three samples, the differences arising from the low-temperature behaviour.

Table 1 lists the OBC% values of the samples at different temperatures ranging from 473 to 773 K. Again, in this case, a parallel behaviour is found between CeTbO_x and Pt/CeTbO_x. For both samples the OBC% values are quite similar in all the temperature ranges. On the other hand, for Rh/CeTbO_x the OBC% is relatively high from 473 K. At 673 K the OBC for Rh/CeTbO_x is >80% whereas for CeTbO_x and Pt/CeTbO_x it is still ~40%. At 773 K, all the samples have similar buffering capacity: close to 100% under the conditions of the experiments.

XPS experiments

For cerium and terbium, the most intense photoemission peak corresponds to the 3d core level. In the case of cerium, most of the XPS data available correspond to the study of the 3d core level.^{19–22,25} For terbium, however, the use of a conventional laboratory spectrometer using Mg or Al K α radiation to analyse the 3d core level will produce photoemitted electrons with very low kinetic energies. This makes it difficult to distinguish accurately between terbium oxidation states in many laboratory instruments. The next most intense core level for terbium is 4d. As shown in Fig. 3(A), Tb 4d XPS spectra are quite complex and it is not easy to determine the oxidation state of terbium. Furthermore, Tb 4d has a binding energy (148.9 eV for 4d_{5/2} in TbO₂) quite different from that of the Ce 3d core level (882.4 eV for 3d_{5/2} in CeO₂), and thus the analysed depth will be necessarily different in each case. This makes it difficult to compare cerium and terbium oxidation states or compositions in the cerium–terbium mixed oxides studied in this paper. Thus, to study Tb 3d spectra and to compare them with those of Ce 3d it was necessary to use synchrotron radiation as the x-ray source for photoemission. For this reason, THE-XPS²⁷ was applied on these samples.

Owing to the fact that papers dealing with Tb 3d XPS are rather scarce, we used two pure terbium oxides as reference. The TbO_{1.5} oxide was prepared by heating a commercial terbium oxide under an inert gas flow at high temperature until full reduction was reached. Composition of the commercial terbium oxide was TbO_{1.82}, as determined by thermogravimetric analysis. The THE-XPS spectra were therefore recorded for TbO_{1.5} oxide, where all terbium ions are in the trivalent oxidation state (Fig. 3(B,a)), and for TbO_{1.82} oxide, where there is a mixture of Tb(III) and Tb(IV) (Fig. 3(B,b)). From the figure, it is evident that the spectra are strongly modified, depending upon the oxidation state of terbium. Thus, as can be seen in Fig. 3(B,a), the Tb³⁺ spectrum shows two doublets, one at 1239.1 and 1274.0 eV (for 3d_{5/2} and 3d_{3/2}, respectively), and the corresponding satellites at 1250.4 and 1286.3 eV. The main photoemission peaks for Tb⁴⁺ appear at 1241.4 eV and 1276.0 eV. In addition to the main peaks, terbium in the tetravalent state shows relatively intense satellites (marked with arrows in Fig. 3(B,b)) at 1251.5 and 1287.7 eV for the 3d_{5/2} and 3d_{3/2} components,

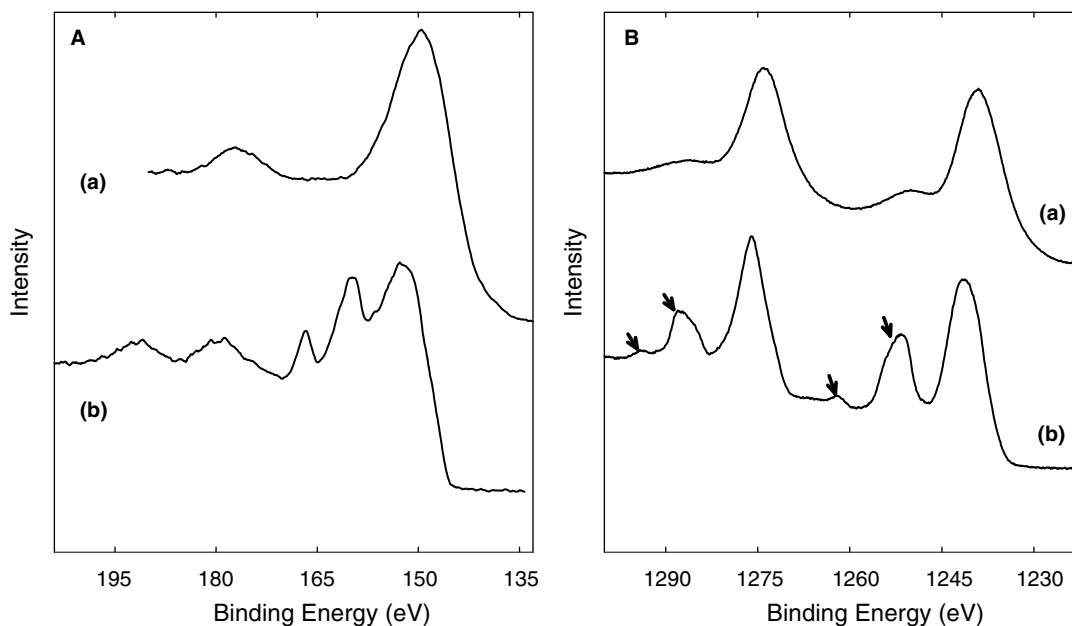


Figure 3. The THE-XPS spectra corresponding to 4d (A) and 3d (B) core levels of two pure terbium oxides: $\text{TbO}_{1.5}$ (100% Tb^{3+} , curves a) and $\text{TbO}_{1.82}$ (36% Tb^{3+} , curves b). The arrows point to the position of the Tb^{4+} satellites.

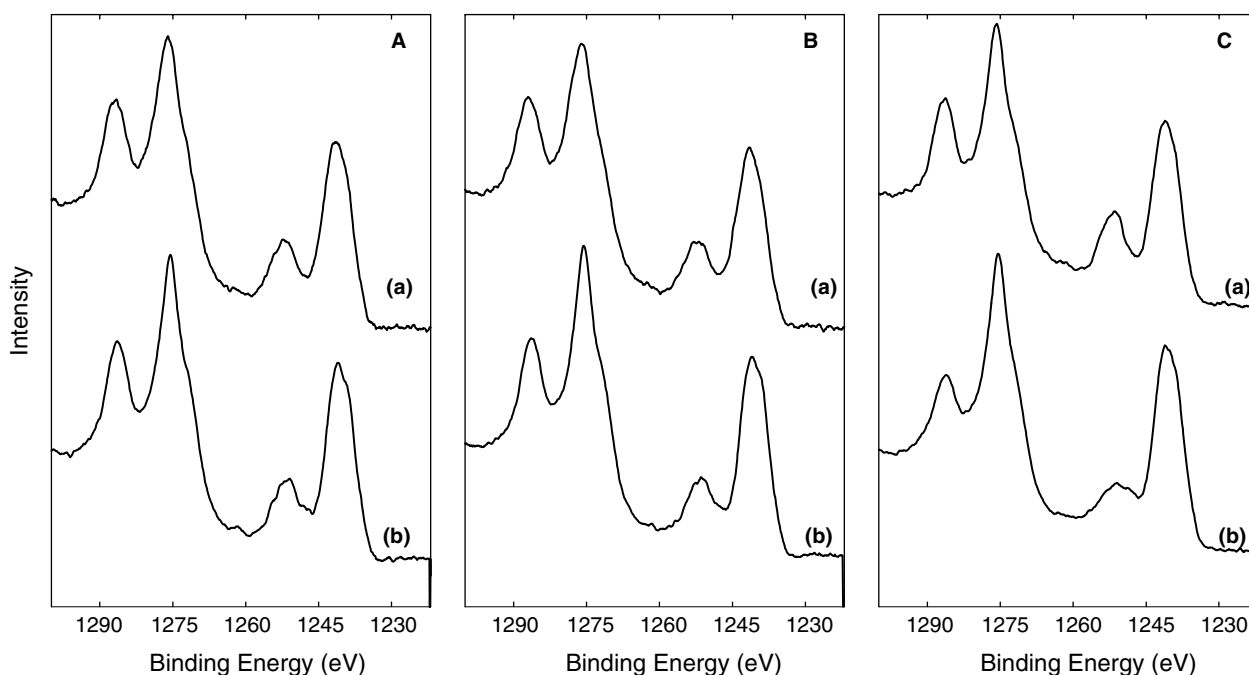


Figure 4. The THE-XPS spectra corresponding to Tb 3d core levels of CeTbO_x (A), Pt/CeTbO_x (B) and Rh/CeTbO_x (C) after the standard oxidizing treatment (curves a) and after UHV at 750 K (curves b).

respectively, accompanied by weaker doublets at 1262.1 and 1294.1 eV. The higher the relative intensity of the satellites, the higher the tetravalent terbium content in the sample.

Taking this into account, we performed THE-XPS experiments on the samples. In Fig. 4, the Tb 3d core levels of the three standardized samples are plotted (trace a). It can be seen that the starting oxidation states of the samples are quite similar, because the relative intensity of the satellite at 1251.5 eV with respect to the main photoemission peak is almost the same in all the cases. It is also worth noting that the $\text{Tb}^{3+}/\text{Tb}^{4+}$ ratio is higher in the mixed oxides than in the reference sample ($\text{TbO}_{1.82}$). Concerning the Ce 3d core

level, no evidence of appreciable amounts of Ce^{3+} could be observed in any of the samples.

The samples were also studied by THE-XPS after being submitted to thermal treatment under UHV at 750 K. Again, the Ce 3d core levels did not show appreciable amounts of Ce^{3+} . The results for Tb 3d core levels are shown in Figs 4(A), 4(B) and 4(C) for CeTbO_x , Pt/CeTbO_x and Rh/CeTbO_x , respectively. By analysing the evolution of the satellite at 1251.5 eV, some deductions can be made: CeTbO_x and Pt/CeTbO_x samples show similar behaviour, having a similar reduction degree when the temperature is raised from 298 to 750 K; Rh/CeTbO_x , however, shows a much

higher reduction degree than the others after being heated at 750 K, and this behaviour is well correlated to that observed in TPD and OBC experiments. From these results, it appears that the improved redox behaviour shown by Rh/CeTbO_x with respect to Pt/CeTbO_x or CeTbO_x can be explained as a promoting effect of rhodium in the reducibility of the mixed oxide when the reduction process proceeds with direct production of O₂, as is the case in TPD. However, when the reduction process depends upon the interaction with hydrogen, as in the TPR experiments, the Pt- and Rh-containing samples show similar behaviour.

CONCLUSIONS

The ability of cerium/terbium mixed oxides to be reduced under inert gas, even at mild temperature, has been reported previously. In such conditions the mixed oxide releases molecular oxygen and the generation of vacancies and reduction from tetravalent to trivalent cations occurs.

When hydrogen is the reducing agent, the reduction proceeds with water evolution. In supported catalysts, noble metals play an important role on the reducibility of ceria and ceria-based mixed oxides. This is related to the ability of the noble metal to activate H₂ molecules.

Accordingly, in this work it can be noticed that the reducibility of CeTbO_x is enhanced when reducing under H₂, both in the Rh- and Pt-containing samples. On the other hand, THE-XPS spectra show that when the reduction proceeds without H₂ the presence of rhodium can reduce Tb⁴⁺ ions to Tb³⁺ to an appreciable extent, thus showing an important promotion of the reducibility of CeTbO_x when the reduction process occurs by means of O₂ evolution. This behaviour contrasts with that of Pt/CeTbO_x, where the Tb³⁺ content is always similar to that of the metal-free CeTbO_x.

The THE-XPS technique has proved to be very useful for studying the actual reduction degree of cerium–terbium mixed oxide, providing information about the redox state of each one of the two cations present in this kind of catalytic support and thus providing some issues to discuss for the role that the noble metal plays on the reducibility of the support.

Acknowledgement

This work has been supported by the CICYT (project no. MAT99-0570).

REFERENCES

1. Trovarelli A, Leitenburg C, Boaro M, Dolcetti G. *Catal. Today* 1999; **50**: 353.
2. Shelef M, McCabe RW. *Catal. Today* 2000; **62**: 35.
3. Kaspar J, Fornasiero P, Graziani M. *Catal. Today* 1999; **50**: 285.
4. Harrison B, Diwell AF, Hallett C. *Platinum Metals Rev.* 1988; **32**: 73.
5. Bernal S, Calvino JJ, Cauqui MA, Gatica JM, Larese C, Pérez-Omil JA, Pintado JM. *Catal. Today* 1999; **50**: 175.
6. Trovarelli A. *Catal. Rev. Sci. Eng.* 1996; **38**: 439.
7. Narula CK, Haack LP, Chun W, Jen HW, Graham GW. *J. Phys. Chem. B* 1999; **103**: 3634.
8. Sinev MY, Graham GW, Haack LP, Shelef M. *J. Mater. Res.* 1996; **11**: 1960.
9. Bernal S, Blanco G, Cauqui MA, Martin AI, Pintado JM, Galtayries A, Sporken R. *Surf. Interface. Anal.* 2000; **30**: 85.
10. Zamar F, Trovarelli A, Leitenburg C, Dolcetti G. *Studi. Surf. Sci. Catal.* 1996; **101**: 1283.
11. Bernal S, Blanco G, Cauqui MA, Corchado MP, Pintado JM, Rodríguez-Izquierdo JM, Vidal H. *Stud. Surf. Sci. Catal.* 1998; **116**: 611.
12. Bernal S, Blanco G, Cauqui MA, Corchado MP, Pintado JM, Rodríguez-Izquierdo JM. *Chem. Commun.* 1997; 1545.
13. Bernal S, Blanco G, Cauqui MA, Corchado MP, Larese C, Pintado JM, Rodríguez-Izquierdo JM. *Catal. Today* 1999; **53**: 607.
14. Tauster SJ, Fung SC, Garten RL. *J. Am. Chem. Soc.* 1978; **100**: 170.
15. Arashi H, Naitoh H, Ishigame M. *Solid State Ionics* 1990; **40/41**: 539.
16. Esteva JM, Karnatak RC, Dexpert H, Gasgnier M, Caro PE, Albert L. *J. Phys.* 1986; **47**: C8–955.
17. Eyring L. *J. Solid State Chem.* 1970; **1**: 376.
18. Bernal S, Blanco G, Calvino JJ, Cifredo GA, Pérez-Omil JA, Pintado JM, Varo A. *Stud. Surf. Sci. Catal.* 1994; **82**: 507.
19. Kotani A, Ikeda T, Okada K, Ogasawara H. *J. Electron Spectrosc. Relat. Phenom.* 1990; **51**: 229.
20. Kotani A, Ogasawara H. *J. Electron Spectrosc. Relat. Phenom.* 1992; **60**: 257.
21. Sarma DD, Rao CNR. *J. Electron Spectrosc. Relat. Phenom.* 1980; **20**: 25.
22. Hu Z, Kaindl G, Müller BG. *J. Alloys Comp.* 1997; **246**: 177.
23. Wuiloud E, Delley B, Schneider, W-D, Baer Y. *Phys. Rev. Lett.* 1984; **53**: 202.
24. Fujimori A. *Phys. Rev. B* 1984; **28**: 4489.
25. Mullins DR, Overbury SH, Huntley DR. *Surf. Sci.* 1998; **409**: 307.
26. Cumpson PJ, Seah MP. *Surf. Interface. Anal.* 1997; **25**: 430.
27. Drube W, Grehk TM, Treusch R, Materlik G. *J. Electron Spectrosc. Relat. Phenom.* 1998; **88-91**: 683.